Construction and Readout Systems for Gaseous Muography Detectors

Dezső Varga,[1,2] Szabolcs J. Balogh,[1] Ádám Gera,[1] Gergő Hamar,[1,2] Gábor Nyitrai,[1,2,3] and Gergely Surányi[4]

[1]*Wigner Research Center for Physics, Budapest, Hungary*
[2]*Virtual Muography Institute*
[3]*Budapest University of Technology and Economics, Budapest, Hungary*
[4]*MTA-ELTE Geological Geophysical SSRG, Budapest, Hungary*

Corresponding author: Dezső Varga
Email: Varga.Dezso@wigner.hu

Abstract

Muography instrumentation presents a wide range of practical challenges since the implementation environment drastically differs from the high energy physics laboratory conditions. This paper briefly overviews the pros and cons of existing technologies, and gaseous detectors in particular. The practical challenges are partially environmental, such as thermal cycling or high humidity, partially connected to the installation such as mechanical shocks, and also include the human factor stipulating minimal non-expert maintenance and troubleshooting. The presentation aims to introduce various solutions to address these challenges, with operational experience spanning five years.

Keywords: muography, gaseous detectors, applied physics
DOI: 10.31526/JAIS.2022.307

1. PARTICLE DETECTORS IN MUOGRAPHY

Muography is a rapidly developing science, originating from high energy physics instrumentation, finding a broad range of applications. The literature expanded considerably [1] in the last decade, which is apparent through a large number of contributors to the present Muographers 2021 Workshop. Even though a full introductory overview does not fit the scope of this paper, some of the well-established applications are worthy of mention. Volcanology was pioneered in Japan [2], and soon various volcanoes have been imaged throughout the world, such as the La Sourfrière [5], Mount Etna [6], and Vesuvius by the MURAVES collaboration [7]. There are various other applications, notably underground imaging such as at Mount Echia [8], and railway tunnel overburden monitoring [9]. A high-profile application targeted the Khufu Pyramid [10]. In terms of methodology, machine learning [11] starts to become a viable tool.

As a response to the demands, muography instrumentation developed accordingly. There are three basic detector technologies differing in the sensitive material. Scintillators are high efficiency and robust detectors [12], which were included in the first practical systems, and are being continuously developed [13]. The second branch is nuclear emulsions, which underwent a renaissance in high energy physics by the turn of the century and was proven to be highly flexible and reliable imaging instruments [15] with the only drawback of lack of real-time monitoring capability. The third group is gaseous detectors [14], which are more complicated and challenging relative to scintillators or emulsions, but more cost-efficient if large areas are required.

With the rapidly increasing number of successful measurement campaigns, it became clear to detector designers that muography instruments require a complete system design, including particularly readout electronics matching the sensor, efficient power supply solutions, tolerance for environmental variations, and possible other forms of supply components (such as working gas for gaseous detector types). The present paper introduces the elements of such self-contained instruments based on multiwire proportional chambers (MWPCs), dedicated to muography.

2. MWPC-BASED MUOGRAPHY DETECTORS

Multiwire proportional chambers, once revolutionized high energy physics, are viable choices as muography tracking detectors [16], given their high detection efficiency, reasonable position resolution, and cost efficiency for large surfaces [17]. In the case of muography applications, major improvements are needed relative to standard high energy physics instrumentation: improved mechanical strength, tolerance for large temperature variations, and lower weight, while maintaining sufficient efficiency at low gas flow [21] (low outgassing and oxygen diffusion). These improvements may be traded for lower rate capability (cosmic muons have very a low rate relative to those in accelerator-based HEP experiments) and increased material budget for the sensitive area

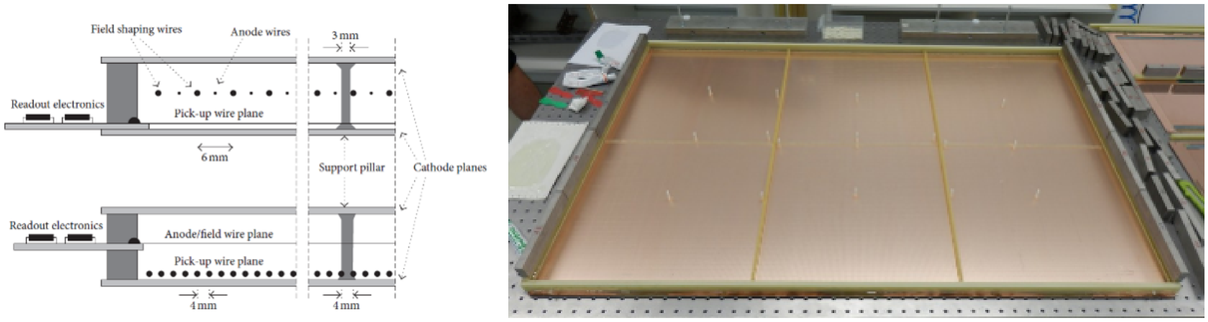

FIGURE 1: MWPC design for muography applications. The structure is shown on the left, with a single HV source on the anode wires, with all other electrodes near ground potential. One chamber just before closing is shown on the right, with internal wire support and pillar structure visible.

(no need, for example, for thin cathode foil). Details on the construction, as well as a chamber before closure, are shown in Figure 1: note the consistent material choice; namely, both cathode and sidewalls are made of glass epoxy (glass fiber reinforced epoxy, same as used in printed circuit boards).

Increasing position resolution drastically increases costs and weakens the mechanical stability of MWPCs, and in order to relax particularly the mechanical tolerances, the Close Cathode Chamber (CCC) [22] has been evaluated as a muography detector [23]. The CCC version is most conveniently constructed with cathode strip pitch of 3-4 mm, resulting in 2-3 mm FWHM position resolution, whereas standard 12 mm pitch MWPCs have 9 mm (FWHM) resolution.

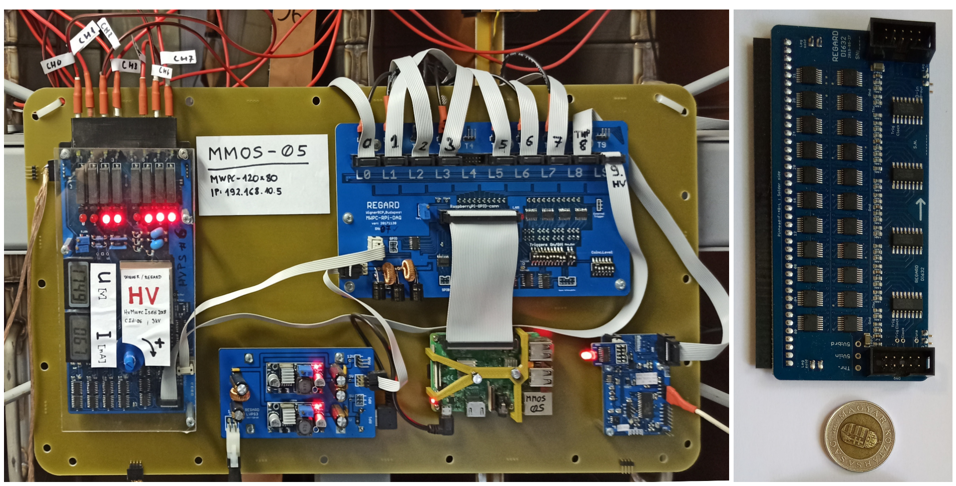

FIGURE 2: Left image: DAQ of an MMOS: RaspberryPi on the bottom middle, high voltage supply on the left, and signal matching and timing board on the top. Right image: front-end cards for MWPC-type detectors with 32 channels.

3. READOUT AND DATA ACQUISITION SYSTEM

The MWPC detectors, introduced in the previous section, have a very convenient feature from the point of view of the signal readout, which can be understood from the cross section (Figure 1). Three types of signals can be extracted from the chambers. One is the summed anode (sense) wires, which can be applied as a good quality trigger. The other is the field shaping wire signal, which gives one coordinate position information (direction perpendicular to the sense wires). The third is the pick-up wires (or printed copper strips in case of the CCC), which is position information parallel to the sense wires. The latter two are both positive, comparable in amplitude, and have very similar pulse shapes. This drastically simplifies the front-end electronics structure, with the same type of front-end readout cards on both coordinates of the Cartesian readout and a single channel for triggering from the anode.

The complete readout system is shown in Figure 2, which is controlled by a single Raspberry Pi microcomputer. The trigger signals are collected from all chambers, and combined to a “master trigger,” usually a condition of at least 3 coincident trigger hits from all (5–8) chambers. For all master triggers, the front-end cards, shown on the right panel of Figure 2, are read out. The system is intentionally simple and robust, which results in a readout (dead) time of around 0.1 ms for each event.

MWPCs require a high voltage supply; for this specific chamber design, the anode voltage is in the range of +1600–+1800 V, at a very low anode dark current. For this purpose, the BPS series of the “iseg” company is a particularly well-suited, low-power module. The high voltage parameters (nominal and measured voltage, as well as measured current) are continuously recorded, along with environmental parameters (temperature, pressure, and humidity).

For remote applications, the total power consumption is an important parameter. The DAQ system presented above [17] consumes 6–9 W power (at 11–15 V unregulated DC voltage). This breaks down as 2-3 W for the Rpi, 2–4 W for the front-ends, and 2-3 W for all other elements.

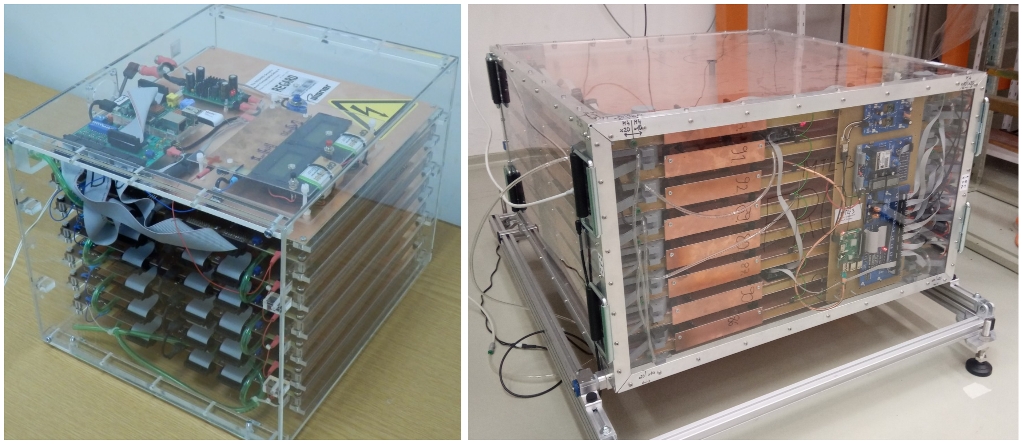

FIGURE 3: Left image: 25 cm size CCC-based compact tracking system. Right image: the “Muon Tomograph Large” version, with 76 cm by 76 cm sensitive area.

FIGURE 4: Detector system compatible with volcanology application, planned to be applied at Etna. The left panel shows the image of the MWPC tracking system, the right panel shows the full proposed setup with a scintillator telescope on top.

4. MUOGRAPH DESIGNS

The muography applications require different detector parameters, and therefore different systems, for various tasks; thus, several designs were developed based on the technologies introduced above. It is a general rule that in muography imaging one fights for statistics. An optimal detector installation position can considerably improve the relevance of the measurement [18], and not all detectors can fit into the optimal place.

Many underground and particularly speleological applications require a simple-to-carry and low power device, which can be transported into natural caves. The “MTS” muograph series are equipped with 6–8 CCC chambers for tracking, weigh less than 5–10 kg, and are not larger than 40 cm (see Figure 3(left)).

In the case of artificial tunnels, or shafts with simple access (e.g., mining, archeology), larger muographs can be used to collect higher statistics. The “MTL” detectors are using $80 \times 80\,\text{cm}^2$ area MWPCs, mounted onto a tiltable stand (see Figure 3(right)).

Volcanology and various surface-based experiments require a near-vertical array of detectors, possibly with several scattering layers included (usually lead plates). The area usually needs to be large due to the low muon flux, which requires firm support. In the case of the Sakurajima Muography Observatory [17], more than 10 individual telescopes work together, each module consists of 7–9 MWPC chambers of size 80–120 cm. A recently planned campaign aims for the Etna volcano, with the combination of complementary gaseous and scintillator [13] technologies, shown in Figure 4.

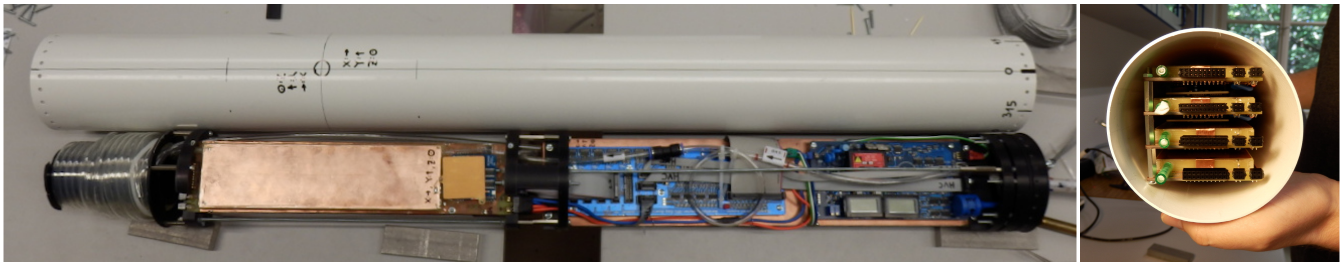

FIGURE 5: Four small-size CCC-based detectors fit into a 100 mm inner diameter tube, along with full readout and DAQ.

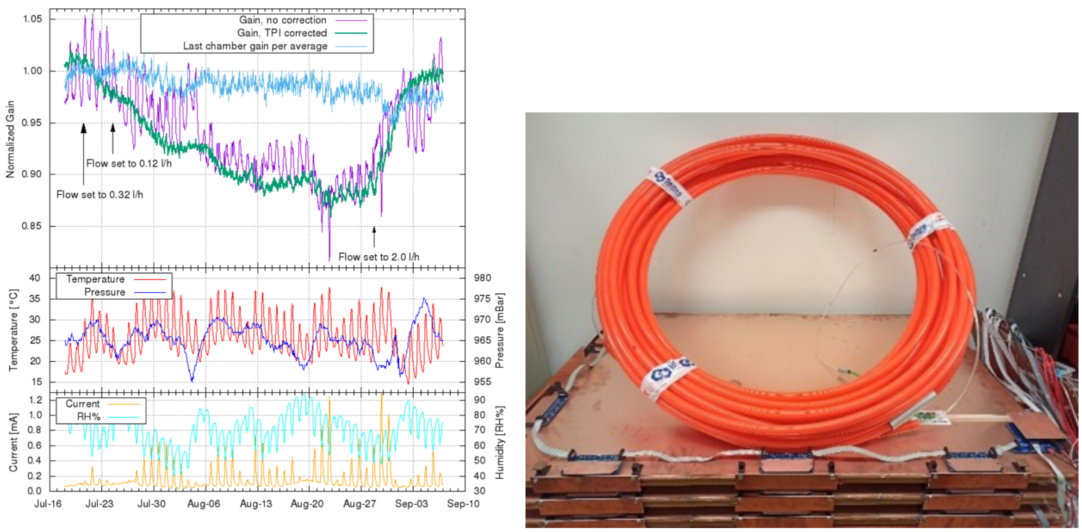

FIGURE 6: Measurement results of an outdoor system with 3 l/day gas flow. The left top panel shows the mean measured gain, reduced only by 10% during the testing, whereas the left bottom panel shows environmental conditions. The key element to act as a buffer for daily temperature cycles is a long, low diffusion tube, shown on the right.

Borehole muography is one of the most challenging tasks, given the limited space and difficult access. A design with 4 pieces of $5 \times 20\,\mathrm{cm}^2$ area CCC chambers and a corresponding DAQ system (see Figure 5) can fit into a 100 mm diameter tube.

5. IMPROVED AUTONOMY WITH REDUCED GAS CONSUMPTION

Gaseous detectors usually run with low but steady gas flow, in order to purge the working gas contamination from external oxygen by diffusion, and outgassing from construction materials. This inherently results in the operational complication of providing gas supply, including necessary maintenance operations of gas cylinder replacement. Various approaches exist to address this [19], including possibly sealed detectors [20]. In order to reduce this gas consumption in the MWPC-based detector systems described above, a detailed study was conducted [21], with the aim of understanding the key factors limiting minimal gas flow. An important practical limitation is due to daily temperature cycles, which reverse the flow at the gas output, and can be eliminated with a sufficiently long buffer volume. A full size (0.9 square meters, 8 chambers) system was operated outdoor for more than 1 month and demonstrated safe running performance at 0.12 l/h (3 l/day) gas flow, as indicated in Figure 6. Such studies pave the way toward low-maintenance muography instruments.

6. UNDERGROUND MUOGRAPHY CAMPAIGNS AND APPLICATIONS

Extensive operational experience has been gathered during actual underground measurements, illustrated by photographs of MWPC-based detectors during installation in Figure 7. A new detector construction is first verified via detailed laboratory measurements, which is followed by shallow-depth underground tests: an example is the Jánossy underground laboratory, a tunnel system at 10–20–30 m depth, located in the Campus of Wigner RCP [25].

Our group was involved in several underground muography campaigns, where the trackers presented above have been used. A summary of these works can be found in [30] while some details are highlighted below.

The Molnár János cave in Budapest is a source of hot springs, where cave structures above the observation point have been searched for [24]. The Ariadne cave system is located in the Pilis mountains, where an unexpected anomaly was found from geoelectric measurements. Muography measurements have been performed from inside the Ajándék cave, and the existence of

FIGURE 7: Underground application examples.

additional cave parts in that region has been excluded [24]. An extensive campaign was performed in the Királylaki cave and tunnel system, with more than 50 locations, and could reveal several density anomalies. The findings have been confirmed via mechanical drilling in 2021, showing low-density erosion zones inside the overburden rock base [27]. Recent focus is toward the Sátorkö-puszta cave system, where multiple measurements were taken with various detectors (depending on where they could fit into); detailed analysis and interpretation are in progress.

Muography measurements were applied as a survey to determine the directional cosmic background in Felsenkeller, near Dresden, where a low-background laboratory was planned [26]. A similar long-term survey has been performed at the MGGL laboratory inside the Mátra mountain at the proposed location of a next-generation gravitational wave detector [28, 29].

CONFLICTS OF INTEREST

The authors declare that there are no conflicts of interest regarding the publication of this paper.

ACKNOWLEDGMENTS

This work has been supported by the Joint Usage Research Project (JURP) of the University of Tokyo, Earthquake Research Institute (ERI), under project ID 2020-H-05, the "INTENSE" H2020 MSCA RISE project under Grant Agreement No. 822185, and the Hungarian NKFIH research grant under ID OTKA-FK-135349 and TKP2021-NKTA-10, the János Bolyai Scholarship of the HAS, and the ELKH-KT-SA-88/2021 grant.

References

[1] H. K. M. Tanaka and L. Oláh, Overview of muographers, Philosophical Transactions of the Royal Society A **377**, 20180143 (2018).
[2] H. K. M. Tanaka et al., Radiographic visualization of magma dynamics in an erupting volcano. Nat. Commun. 5, 3381 (2014).
[3] H. K. M. Tanaka, K. Sumiya, and L. Oláh, Muography as a new tool to study the historic earthquakes recorded in ancient burial mounds. Geoscientific Instrumentation, Methods and Data Systems **9**, 357 (2020).
[4] L. Oláh and H. K. M. Tanaka, Muography of Magma Intrusion Beneath the Active Craters of Sakurajima Volcano, Japan. Geophysical Monograph Series **270**, 109 (2022).
[5] K. Jourde et al., Muon dynamic radiography of density changes induced by hydrothermal activity at the La Soufrière of Guadeloupe volcano. Sci. Rep. 6 p (2016).
[6] D. LoPresti et al., Muographic monitoring of the volcano-tectonic evolution of Mount Etna, Sci. Rep. 10 p11351 (2020).
[7] G. Bonomi et al., Applications of cosmic-ray muons, Prog. Part. Nucl. Phys. 112, p103768 (2020).
[8] G. Saracino et al., Imaging of underground cavities with cosmic-ray muons from observations at Mt. Echia (Naples), Sci. Rep. 7, 1187 (2017).
[9] L. F. Thompson et al., Muon tomography for railway tunnel imaging, Phys. Rev. Research 2, 023017 (2020).
[10] K. Morishima et al., Discovery of a big void in Khufu's Pyramid by observation of cosmic-ray muons, Nature 552, 386–390 (2017).
[11] L. Oláh and H. K. M. Tanaka, Machine Learning with Muographic Images as Input: An Application to Volcano Eruption Forecasting. Geophysical Monograph Series **270**, 43 (2022).
[12] F. Ambrosino et al., The MU-RAY project: detector technology and first data from Mt. Vesuvius, JINST 9 C02029 (2014).
[13] D. Lo Presti et al., The MEV project: Design and testing of a new high-resolution telescope for muography of Etna Volcano, NIM A 904, 195–201 (2018).
[14] S. Bouteille et al., A Micromegas-based telescope for muon tomography: The WatTo experiment, NIM A 834, 223–228 (2016).
[15] K. Morishima et al., Development of nuclear emulsion for muography, Ann. Geophys. 60, S0112 (2017).
[16] D. Varga et al., High Efficiency Gaseous Tracking Detector for Cosmic Muon Radiography. AHEP 2016, 1962317.
[17] L. Oláh et al., High-definition and low-noise muography of the Sakurajima volcano with gaseous tracking detectors, Sci. Rep. 8 3207 (2018).

[18] Leone Giovanni et al., Muography as a new complementary tool in monitoring volcanic hazard: implications for early warning systems. Proc. R. Soc. A.4772021032020210320 (2021).
[19] S. Procureur et al., Why do we flush gas in gaseous detectors?, Nucl. Instrum. Methods Phys. Res., Sect. A 955, 163290 (2020).
[20] L. Lopes et al., Towards sealed resistive plate chambers, J. Instrum. 15, C11009 (2020).
[21] G. Nyitrai et al., Towards low gas consumption of muographic tracking detectors in field applications, J. Appl. Phys. 129, 244901 (2021).
[22] D. Varga, G. Hamar, G. Kiss, and G. Bencedi, Close Cathode Chamber: Low material budget MWPC. Nucl. Instrum. Meth. A 698, 11 (2013).
[23] G. G. Barnaföldi et al., Portable Cosmic Muon Telescope for Environmental Applications, Nucl.Instrum.Meth. A 689, 60 (2012).
[24] L. Oláh et al., CCC-based Muon Telescope for Examination of Natural Caves. Geosci. Instrum. Method. Data Syst. 1, 229 (2012).
[25] L. Oláh et al., Applications of cosmic muon tracking at shallow depth underground, ICATPP 2013, 280 (2014).
[26] L. Oláh et al., Cosmic background measurements at a proposed underground laboratory by the REGARD Muontomograph, Journal of Physics Conf.Ser. 665, 012032 (2015).
[27] G. Surányi et al., Locating of density anomalies using highly penetrating cosmic muons, Karsztfejlodés 2016, 203 (2016).
[28] P. Ván et al., First report of long term measurements of the MGGL laboratory in the Márta mountain, Classical and Quantum Gravity 34, 114001 (2017).
[29] P. Ván et al., Long term measurements from the Mátra Gravitational and Geophysical Laboratory, European J. Phyisics ST 228, 1693 (2019).
[30] Muography: Exploring Earth's Subsurface with Elementary Particles: Chapter 11, Wiley AGU Books, 2022.